J. Plasma Fusion Res. SERIES, Vol. 5 (2002) 342–345

Behavior of Intrinsic and Injected Impurities in Heliotron J ECH Plasmas

KAWAZOME Hayato, MAENO Shogo, KONDO Katsumi, IRIGUCHI Masao, TAKEDA Masafumi, MIZUUCHI Tohru[1], OKADA Hiroyuki[1], NAGASAKI Kazunobu[1], SANO Fumimichi[1], BESSHOU Sakae, MANABE Yoshito, SHIDARA Hiroyuki, ANG Wan Leng, TAKAMIYA Tasho, TSURU Hiroki, TOMIYAMA Keishi, OHNO Yoshinori, KUBO Hiroyasu, NISHIOKA Yusuke, YUKIMOTO Hidetoshi and OBIKI Tokuhiro[1]

Graduate School of Energy Science, Kyoto University, Gokasho, Uji 611-0011, Japan

[1] *Institute of Advanced Energy, Kyoto University, Gokasho, Uji 611-0011, Japan*

(Received: 11 December 2001 / Accepted: 15 July 2002)

Abstract

The behavior of impurities is studied for Heliotron J ECH plasmas using VUV and visible spectrometers. Plasmas are produced by 70 GHz ECH. In VUV spectra, oxygen (O III, O IV, O VI), carbon (C III, C IV), titanium (Ti XI, Ti XII), iron (Fe XV, Fe XVI) and chromium (Cr XIII, Cr XIV) are identified as typical impurities. For impurity injection experiments, movable gas puff system is installed in Heliotron J. Preliminary spectroscopic results of helium gas injection into the plasma are presented.

Keywords:

Heliotron J, impurity behavior, VUV spectra, impurity injection

1. Introduction

In a study of magnetically confined plasma, generating high temperature plasma is one of the main issues. Impurities in a fusion plasma play a crucial role through radiation losses and the dilution of fuel. It is important to understand the intrinsic impurity species and their behavior. Also it is important to study impurity transport and impurity control with injection experiments.

Heliotron J is a medium sized helical-axis heliotron device with L = 1 and M = 4 [1,2]. The various magnetic configurations can be formed for the study of particle and impurity control, i.e. helical divertor and island divertor configuration [3]. In previous study, hydrogen plasmas are produced by 53 GHz ECH with the injected power of 400 kW in the magnetic field strength from 0.85 T $\leq B \leq$ 1.35 T and two effective heating regions are observed [4]. Recently 70 GHz ECH system with focused incident beam is installed.

In this paper, the behavior of intrinsic and injected impurities are investigated for Heliotron J ECH plasmas using VUV and visible monochromators. The spectrometers are viewing the center of plasma and used to identify impurities and temporally resolved spectral intensity emitting from VUV and visible wavelength region. The identified typical impurities in Heliotron J ECH plasmas will be described in Sec. **2**. Section **3** describes the preliminary spectroscopic results of helium injection into the plasma by the movable gas puff system. The last section gives summaries.

2. Behavior of Intrinsic Impurities in a Heliotron J ECH Plasma

Behavior of intrinsic impurity species in Heliotron J ECH plasmas is studied. VUV spectra are measured

Corresponding author's e-mail: kawazome@center.iae.kyoto-u.ac.jp

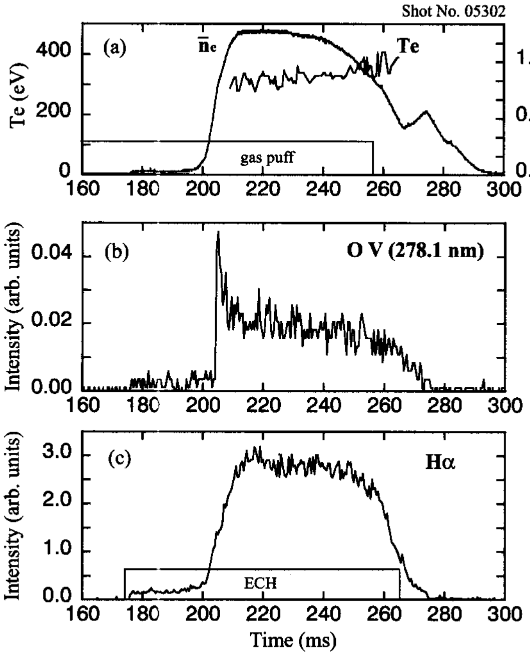

Fig. 1 The temporal evolution of the discharge in standard configuration (B = 1.28 T). The plasma is produced by the 70 GHz ECH: (a) the line average electron density and the electron temperature, (b) line intensity of O V (278.1 nm), (c) line intensity of H_α.

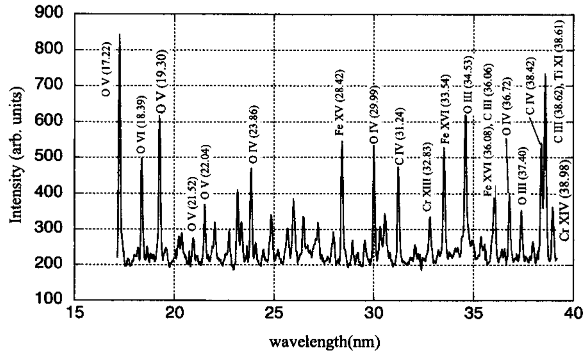

Fig. 2 VUV spectra at t = 215 ms in shot No. 5302. Identified spectra are indicated by their species and wavelength in nm.

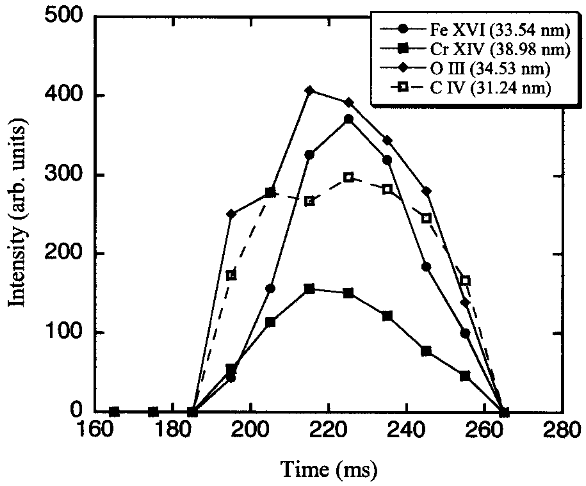

Fig. 3 Time-resolved line intensity in shot No. 5302.

with using a time-resolving grazing incident spectrometer with a multichannel detector [5]. Wavelengths of observed spectra are ranged from 15 nm to 40 nm, the minimum time resolution is 10 ms and the wavelength resolution is approximately 0.1 nm.

Plasmas are produced by the 70 GHz ECH with the power of 400 kW and the pulse width is 80 ms. Figure 1 shows a temporal evolution of the discharge in standard configuration (B = 1.28 T). The line average electron density and the electron temperature are evaluated from a microwave interferometer and a soft x-ray filter absorption method, respectively. The electron density and the electron temperature are almost constant from 210 ms to 240 ms. Figure 2 shows VUV spectra at t = 215 ms. Figure 3 shows time-resolved plot of Fe XVI (33.54 nm), Cr XIV (38.98 nm), O III (34.53 nm) and C IV (31.24 nm) line intensities in the same discharge. The spectrometer has not been absolutely calibrated and Fig. 3 shows only time evolution of the individual line intensity. These intensities are peak values by subtracting the background. In Fig. 3, O III and C IV lines are observed at 185 ms and the intensities increase because of ionization phase. For metallic impurities, Fe XVI and Cr XIV, increase of the charge state population causes increase in the intensities. After 230 ms, all line intensities decrease with density decrease. In this phase, the electron temperature is almost constant. So it is expected that the electron density decreases with keeping its profile. As the typical intrinsic impurity, oxygen (O III, O IV, O V, O VI), carbon (C III, C IV), titanium (Ti XI, Ti XII), iron (Fe XV, Fe XVI) and chromium (Cr XIII, Cr XIV) are identified. Table 1 shows the identified spectra in Heliotron J ECH plasmas.

3. Helium Gas Injection

In this section we present some preliminary spectroscopic results of helium injection experiment. To investigate the effect of the edge plasma on the impurity

Table 1 Identified typical intrinsic spectra in the Heliotron J ECH plasmas.

Wavelength (nm)	Species	Transition		
17.22	O V	$2s^2\,{}^1S_0$	–	$2s3p\,{}^1P_1^o$
18.39	O VI	$2p\,{}^2P_{1/2}^o$	–	$3s\,{}^2S_{1/2}$
19.30	O V	$2s2p\,{}^3P_2^o$	–	$2s3d\,{}^3D_3$
21.52	O V	$2s2p\,{}^3P_2^o$	–	$2s3s\,{}^3S_1$
22.04	O V	$2s2p\,{}^1P_1^o$	–	$2s3d\,{}^1D_2$
23.86	O IV	$2s^22p\,{}^2P_{3/2}^o$	–	$2s^23d\,{}^2D_{5/2}$
28.42	Fe XV	$3s^2\,{}^1S_0$	–	$3s3p\,{}^1P_1^o$
29.99	O IV	$2s2p^2\,{}^2P_{3/2}$	–	$2s2p({}^3P^o)3d\,{}^2P_{3/2}^o$
31.24	C IV	$2s\,{}^2S_{1/2}$	–	$3p\,{}^2P_{3/2}^o$
32.83	Cr XIII	$3s^2\,{}^1S_0$	–	$3s3p\,{}^1P_1^o$
33.54	Fe XVI	$3s\,{}^2S_{1/2}$	–	$3p\,{}^2P_{3/2}^o$
34.53	O III	$2s^22p^2\,{}^1S_0$	–	$2s^22p3d\,{}^1P_1^o$
36.06	C III	$2s2p\,{}^3P_1^o$	–	$2p3p\,{}^3P_0$
36.08	Fe XVI	$3s\,{}^2S_{1/2}$	–	$3p\,{}^2P_{1/2}^o$
36.72	O IV	$2s^2p^2\,{}^2P_{3/2}$	–	$2s2p({}^3P^o)3s\,{}^2P_{3/2}^o$
37.40	O III	$2s^2p^2\,{}^3P_2$	–	$2s^22p3s\,{}^3P_1^o$
38.41	C IV	$2p\,{}^2P_{3/2}^o$	–	$3d\,{}^2D_{5/2}$
38.61	Ti XI	$3s^2\,{}^1S_0$	–	$3s3p\,{}^1P_1^o$
38.62	C III	$2s^2\,{}^1S_0$	–	$2s3p\,{}^1P_1^o$
38.98	Cr XIV	$3s\,{}^2S_{1/2}$	–	$3p\,{}^2P_{3/2}^o$

penetration into the core region and the influence of the penetrated impurity on plasma performance, a movable gas puff system is installed in Heliotron J. The distance between the top of nozzle and the last closed magnetic flux (LCMF) can be varied. The nozzle is set toward the magnetic axis.

Plasmas are produced by the 70 GHz ECH in the standard configuration (B = 1.26 T). The pulse width and the injected power are 100 ms and 400 kW, respectively. To observe the influence of injected impurity, a low density plasma is produced. The nozzle is located at 60 mm outside the LCMF. Figure 4 shows a temporal evolution of the line average electron density, the electron temperature, and He I and He II intensities in the helium gas injected discharge. The helium gas is injected at 233 ms and turned off at 244 ms. He I and He II line intensities are measured by two monochromators viewing top of nozzle and located at 45 degrees in the toroidal direction from the port of helium injection, respectively. He I and He II line intensities quickly peak in 10 ms after helium is injected and then decays exponentially as a result of further ionization and particle loss. The estimated ionization time from He I to He II in this case is 0.42 ms. The electron temperature and density of the edge region, which are measured with movable probe, are 30 eV and 3×10^{17} m^{-3}, respectively. Injection of helium gas causes increase in the electron density from 1.4×10^{18} m^{-3} to 2.7×10^{18} m^{-3} and decrease in the electron temperature from 0.75 keV to 0.45 keV.

Figure 5 shows time-resolved line intensity of Fe XVI (33.54 nm), Fe XV (28.42 nm) and O III (34.53 nm). After helium gas was injected, intensities increase with increasing the electron density. The electron density and Fe XVI, Fe XV and O III intensities increase 1.9 times, 2.2 times, 6 times and 1.6 times, respectively. O III ions present in the cooler edge region and decrease of electron temperature dose not affect its ionization balance. On the other hand, with decreasing the electron temperature, the recombination and ionization rates of Fe XVI ions, which are present in the core region, increases and decreases, respectively. According to the ionization balance, Fe XVII exists before helium gas injection. It is not confirmed experimentally because of the wavelength of Fe XVII resonance line is shorter than the available wavelength region of the spectrometer. When the electron temperature decreases, Fe XVII and Fe XVI recombine and Fe XV becomes the most abundant ion. In this discharge, decay time of the He II line intensity is about 13 ms.

To investigate the relation between the behavior of

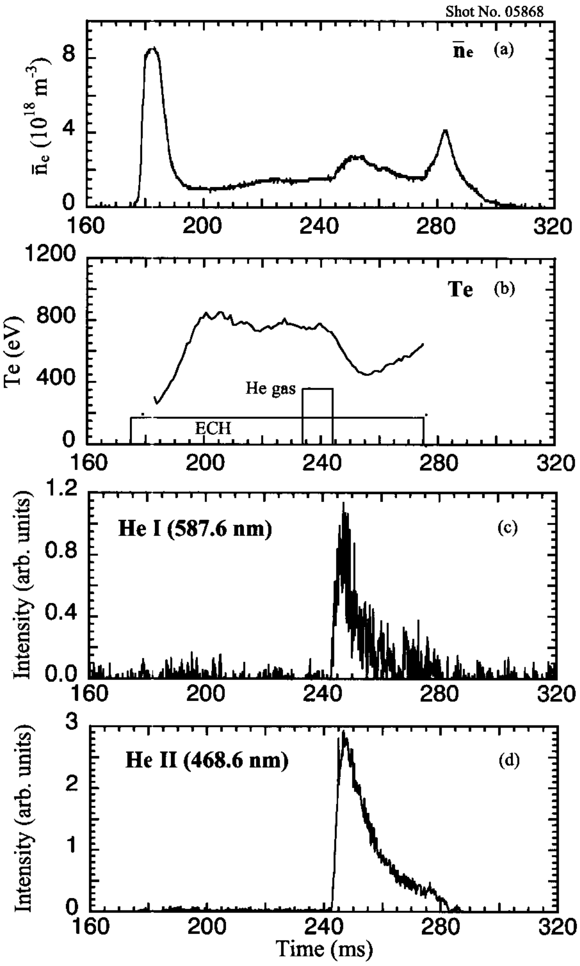

Fig. 4 The temporal evolution of the discharge with helium gas injection: (a) the line average electron density, (b) the electron temperature, (c) line intensity of He I (587.6 nm), (d) line intensity of He II (468.6 nm).

injected impurity and plasma conditions, we performed electron density scan (0.17×10^{19} m^{-3} $\leq n_e \leq 2.2 \times 10^{19}$ m^{-3}) in standard configuration. The dependence of decay time of He I and He II line intensity is not observed clearly. On the other hand He II line intensity normalized by the electron density, which indicates the particle number of helium ions penetrated into the core plasma region, increases with decreasing the electron density. We guess this result arises from the screening effect due to electron collisional ionization at the edge region.

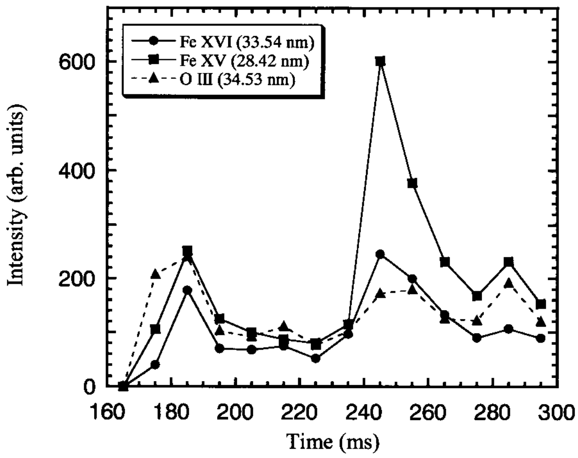

Fig. 5 Time-resolved line intensity with helium gas injection (#05868).

4. Summary

The study of impurity behavior in Heliotron J ECH plasmas has been started with spectroscopic methods. For ECH plasmas, typical impurity species identified by VUV spectra are oxygen, carbon, iron, chromium and titanium. It is considered that these impurities are released from the vacuum vessel wall by desorption and sputtering processes.

In impurity injection experiments, helium gas is injected by movable gas puff system. Helium decay time is obtained as about 13 ms from He II line. In electron density scan, the particle number of ions penetrated into core plasma depends on the electron density. It seems the screening effect due to electron collisional ionization at the edge region.

References

[1] M. Wakatani *et al.*, Nucl. Fusion **40**, 560 (2000).
[2] T. Obiki *et al.*, Plasma Phys. Control. Fusion **4**, 1151 (2000).
[3] T. Mizuuchi *et al.*, J. Nucl. Mater. **290–293**, 678–682 (2001).
[4] T. Obiki *et al.*, Nucl. Fusion **41**, 883 (2001).
[5] K. Kondo *et al.*, Jpn. J. Appl. Phys. **27**, 2368 (1988).